Table 1S. Z-Matrix and Optimized Geometry of HMHP-A CCSD(T)/aug'-cc-pVTZ [a]

O1						
C1	1	R2				
H1	1	R3	2	A3		
H2	2	R4	1	A4	3	D4
H3	2	R5	1	A5	4	D5
O2	2	R6	1	A6	4	D6
O3	6	R7	2	A7	1	D7
H4	7	R8	6	A8	2	D8

Variables:

R2	=	1.39543173
R3	=	0.96375469
R4	=	1.09476547
R5	=	1.08985693
R6	=	1.41221324
R7	=	1.46158782
R8	=	0.96699084
A3	=	107.27260324
A4	=	111.49545679
A5	=	107.51454293
A6	=	113.20334702
A7	=	104.91276565
A8	=	99.90380078
D4	=	-55.01004630
D5	=	-122.36494810
D6	=	123.33384465
D7	=	-68.85675108
D8	=	-113.21992691

[a]Bondlengths in Å and angles in degrees.

Table 2S. Z-Matrix and Optimized Geometry of HMHP-B CCSD(T)/aug'-cc-pVTZ [a]

O1						
C1	1	R2				
H1	1	R3	2	A3		
H2	2	R4	1	A4	3	D4
H3	2	R5	1	A5	4	D5
O2	2	R6	1	A6	4	D6
O3	6	R7	2	A7	1	D7
H4	7	R8	6	A8	2	D8

Variables:

R2	=	1.40733192
R3	=	0.96339276
R4	=	1.08884238
R5	=	1.09334635
R6	=	1.40552024
R7	=	1.45408055
R8	=	0.96951284
A3	=	107.90384486
A4	=	106.40112372
A5	=	112.30573392
A6	=	112.27051255
A7	=	106.33097451
A8	=	100.88706194
D4	=	168.82143771
D5	=	-122.68839050
D6	=	120.89328016
D7	=	-69.80055250
D8	=	74.84944320

[a]Bondlengths in Å and angles in degrees.

Table 3S. Z-Matrix and Optimized Geometry of HMHP-C CCSD(T)/aug'-cc-pVTZ [a]

O1						
C1	1	R2				
H1	1	R3	2	A3		
H2	2	R4	1	A4	3	D4
H3	2	R5	1	A5	4	D5
O2	2	R6	1	A6	4	D6
O3	6	R7	2	A7	1	D7
H4	7	R8	6	A8	2	D8

Variables:

R2	=	1.39940348
R3	=	0.96255148
R4	=	1.09317589
R5	=	1.08958582
R6	=	1.40998762
R7	=	1.46081012
R8	=	0.96704776
A3	=	107.46217459
A4	=	111.37328011
A5	=	107.74235912
A6	=	113.35758969
A7	=	105.06243862
A8	=	99.68649754
D4	=	-43.23496918
D5	=	-122.52535174
D6	=	123.38100855
D7	=	-70.41308955
D8	=	-246.04086240

[a]Bondlengths in Å and angles in degrees.

Figure 1S. FTIR spectrum of HMHP using extended KBR beamsplitter, 1000-4000 cm^{-1}. Supplemental file "HMHP_1000_4000_cm-1.txt" contains the raw data for this plot.

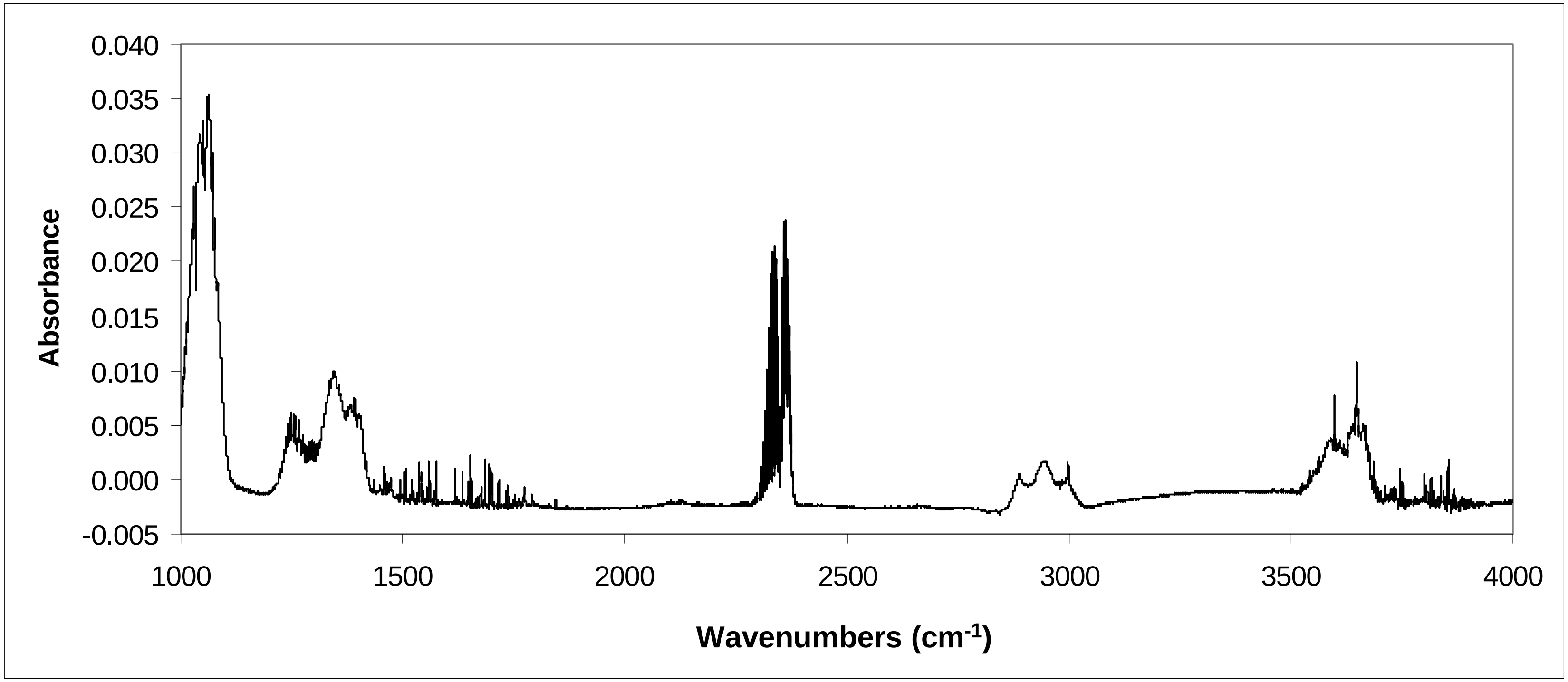

Figure 2S. FTIR spectrum of HMHP using extended CaF_2 beamsplitter, 3500-7500 cm^{-1} (black). FTIR spectrum of H_2O_2 is shown for reference (grey). Supplemental file “HMHP_3500_7500_cm-1.txt” contains the raw data for the HMHP spectrum in this plot.

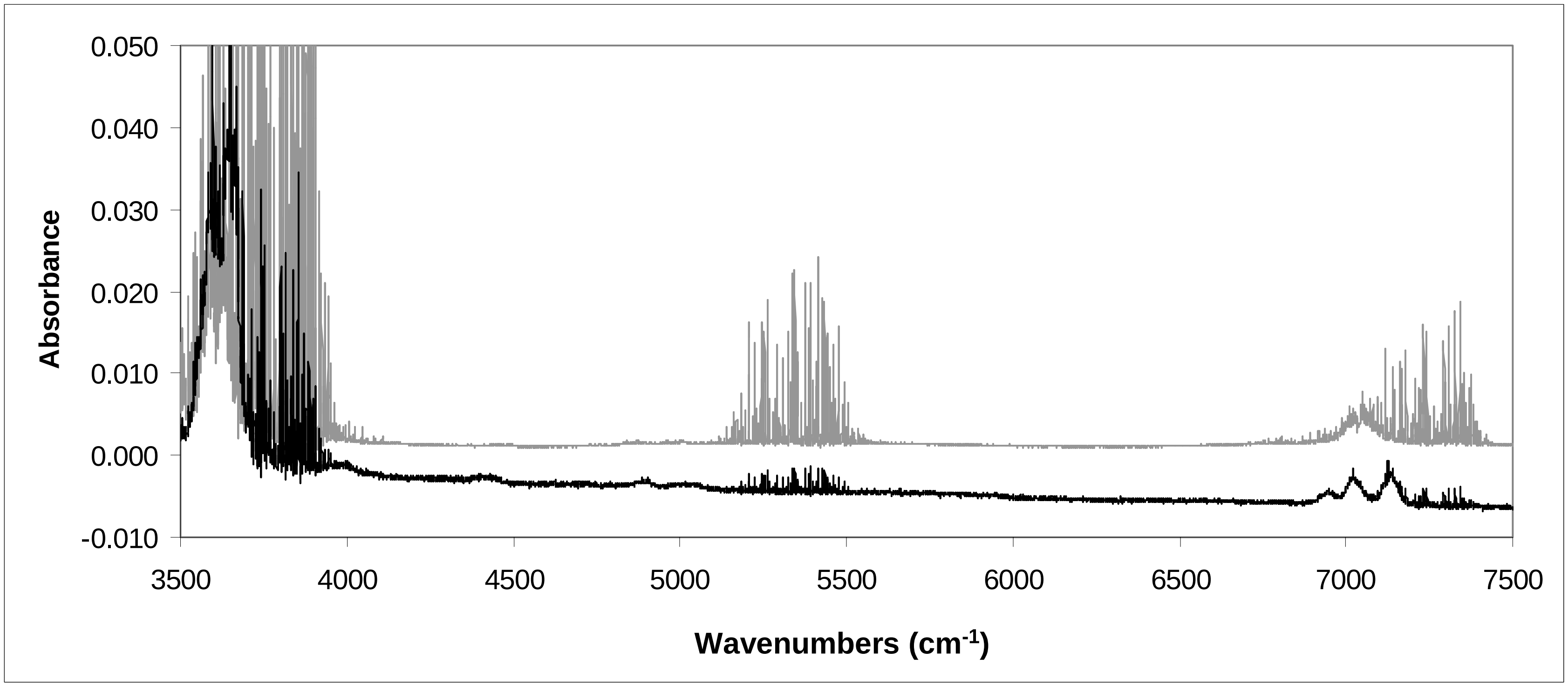

Table 4S. Observed band positions and relative strengths.

Origin	Band center from Niki et al. (cm^{-1})	Band center (cm^{-1})	Relative intensities[a]
C-O stretch	1050	1049.5	2.7
OO-H bend	1350	1344.9	0.9
		2893.2	
C-H stretch	2900	2947.2	0.4
		2999.8	
O**O-H** stretch	3598.1	3598.1	0.7
R**O-H** stretch	3647.8	3647.8	1.0
O-H first		6947.1	.02
overtone		7022.9	.06
region		7125.4	.07

[a]Relative intensities are obtained across the entire spectral range by normalizing to the peak height of the RO-H band in the two FTIR spectra shown in the supplemental material. For the 1000-4000 cm^{-1} bands, an extended KBr beamsplitter was used, for 4000-8000 cm^{-1}, a CaF_2 beamsplitter was used. Niki, H.; Maker, P. D.; Savage, C. M.; Breitenbach, L. P. *Chemical Physics Letters* **1980**, *75*, 533.

Table 5S. Calculated normal mode frequencies (cm^{-1}) and oscillator strengths for HMHP-A, HMHP-B and HMHP-C.[a]

HMHP-A		HMHP-B		HMHP-C	
$\tilde{\nu}$	f	$\tilde{\nu}$	f	$\tilde{\nu}$	f
170	2.3×10^{-7}	173	4.6×10^{-6}	178	4.2×10^{-6}
248	1.4×10^{-5}	311	1.4×10^{-5}	222	3.5×10^{-5}
353	1.7×10^{-5}	392	1.6×10^{-5}	386	1.8×10^{-6}
462	1.2×10^{-5}	438	1.3×10^{-5}	450	5.8×10^{-6}
615	4.5×10^{-6}	635	3.7×10^{-6}	624	2.0×10^{-6}
894	5.3×10^{-6}	907	4.1×10^{-6}	900	4.9×10^{-6}
1046	4.2×10^{-6}	1061	1.6×10^{-5}	1056	4.9×10^{-6}
1097	1.4×10^{-5}	1085	7.2×10^{-6}	1087	1.5×10^{-5}
1132	3.0×10^{-5}	1111	2.2×10^{-5}	1119	3.0×10^{-5}
1309	1.1×10^{-6}	1302	4.4×10^{-6}	1303	2.7×10^{-6}
1379	9.3×10^{-6}	1399	9.2×10^{-7}	1400	8.5×10^{-6}
1416	2.5×10^{-6}	1419	1.1×10^{-5}	1415	3.3×10^{-6}
1451	1.0×10^{-5}	1447	6.9×10^{-6}	1444	6.3×10^{-6}
1517	2.2×10^{-7}	1517	6.4×10^{-7}	1517	4.8×10^{-7}
3056	9.6×10^{-6}	3082	6.2×10^{-6}	3074	7.4×10^{-6}
3154	2.6×10^{-6}	3162	2.7×10^{-6}	3159	2.5×10^{-6}
3814	7.9×10^{-6}	3783	5.4×10^{-6}	3815	7.9×10^{-6}
3862	8.3×10^{-6}	3860	7.8×10^{-6}	3875	7.6×10^{-6}

[a]Calculated at the QCISD/aug’-cc-pVTZ optimized geometry. The frequencies are unscaled.